Deep trapping of electrons by oblique shock waves

Atsushi Zindo and Yukiharu Ohsawa[a)]
Department of Physics, Nagoya University, Nagoya 464-8602, Japan

Naoki Bessho
Department of Physics, The University of New Hampshire, Durham, New Hampshire 03824

Richard Sydora
Department of Physics, University of Alberta, Edmonton, Alberta T6G 2J1, Canada

(Received 9 December 2004; accepted 22 March 2005; published online 9 May 2005)

The mechanism of electron trapping by an oblique shock wave is studied with theory and particle simulations. An energy equation is derived, which focuses on particle velocity and electric field parallel to the magnetic field $\boldsymbol{B}$. It is then shown that electrons can be reflected by a negative dip of F, where F is the integral of the parallel electric field, $E_{\parallel}=(\boldsymbol{E}\cdot\boldsymbol{B})/B$, along $\boldsymbol{B}$. The parallel energy is decreased after the reflection owing to the recovery of F to positive values. This leads to deep electron trapping. These theoretical predictions are verified with relativistic, electromagnetic particle simulations. © *2005 American Institute of Physics*. [DOI: 10.1063/1.1909198]

I. INTRODUCTION

It has recently been shown with particle simulations that a magnetosonic shock wave propagating obliquely to an external magnetic field can accelerate some electrons to ultrarelativistic energies with the Lorentz factor $\gamma>100$.[1–3] (For the acceleration mechanisms of other particle species, see, for instance, Refs. 4–25.) In this mechanism, electrons that are reflected near the end of the main pulse of the shock wave are then trapped and energized in the main pulse region. According to the theory,[1] the reflection occurs when a negative dip of F is formed, where $F=-\int E_{\parallel}ds$ with $E_{\parallel}$ being the electric field parallel to the magnetic field $\boldsymbol{B}$ and ds the infinitesimal length along $\boldsymbol{B}$.

This acceleration mechanism is different from that of the surfatron acceleration, where the longitudinal electric field E_x in an external magnetic field B_{z0} accelerates particles along the wave front. The surfatron acceleration was first suggested by Sagdeev in Ref. 9 and discussed in detail in Refs. 10–12. Katsouleas and Dawson then argued that unlimited acceleration could occur if $E_x/B_{z0}>1$. (For a recent review on the surfatron acceleration, see Ref. 14 and references therein.)

Simulations on the present acceleration mechanism[1–3] show that reflected electrons are trapped deeply, oscillating in the main pulse region where F is large. Reflected electrons move forward and have their maximum energies near the position where F has its maximum value in the main pulse (near this position, the electric potential and magnetic field have also their maximum values). Then, they are reflected backward in the shock transition region. They do not go away ahead of the wave. Also, they do not pass through the shock wave to the downstream region, even if F has been restored to positive values in the end of the main pulse when they return there. Once electrons are reflected, they can hardly escape from the wave.

The reason for the deep electron trapping is unclear. In the present paper, we study this mechanism.

In Sec. II, we analytically discuss the trapping mechanism of electrons. On the basis of the drift approximation, we derive an equation for the energy $\varepsilon=m_e v^2/2-\mu B-eF$, where $m_e v^2/2$ is the electron kinetic energy and μ is the magnetic moment. This energy mainly consists of velocity and electric field parallel to the magnetic field. We then show that the recovery of F from negative to positive values in the end of the main pulse can cause the decrease of the energy ε of the reflected particles. This gives rise to the deep trapping of electrons; just as a particle oscillating in a potential well with damping. Also, we verify that the present energy equation is equivalent to that discussed in Refs. 1–3.

In Sec. III, by using one-dimension (one space coordinate and three velocity components), relativistic, electromagnetic particle simulations, we investigate particle motions in oblique shock waves. It is directly shown that the electron reflection takes place when F has a negative dip in the end of the main pulse. The recovery time of F is much shorter than the oscillation period of trapped electrons. Hence, right after the reflection, the values of F begin to go up around the region where the negative dip was present. It is then shown that the energies of reflected particles decrease.

Section IV gives a summary of our work.

II. THEORY OF ELECTRON TRAPPING

Here, we analytically discuss electron trapping in an oblique shock wave. To obtain the amount of energy that reflected electrons can gain, we need to use the relativistic equation of motion.[3] To qualitatively understand the trapping mechanism, however, we can use a simplified model; we consider nonrelativistic electrons with drift approximation.

In the following, we assume that the waves are one dimensional, $\partial/\partial y=\partial/\partial z=0$, and that their space and time variations are much slower than the electron gyromotion.

[a)]Electronic mail: ohsawa@nagoya-u.jp

The external magnetic field is in the (x,z) plane, $\boldsymbol{B}_0 = (B_{x0}, 0, B_{z0})$.

A. Energy equation

We derive an energy equation for electrons to discuss their motions. In the drift approximation,

$$\boldsymbol{v} = v_{\parallel}\frac{\boldsymbol{B}}{B} + c\frac{\boldsymbol{E}\times\boldsymbol{B}}{B^2} + \tilde{\boldsymbol{v}}, \tag{1}$$

where $\tilde{\boldsymbol{v}}$ is the gyration velocity, we have

$$\boldsymbol{E}\cdot\boldsymbol{v} = \frac{\boldsymbol{E}\cdot\boldsymbol{B}}{B}v_{\parallel} + \boldsymbol{E}\cdot\tilde{\boldsymbol{v}}. \tag{2}$$

Accordingly, with the aid of the relation[26]

$$-e\langle\boldsymbol{E}\cdot\tilde{\boldsymbol{v}}\rangle = \frac{d}{dt}(\mu B), \tag{3}$$

where the brackets denote the time average over a gyroperiod and μ is the magnetic moment, $\mu = m_e\tilde{v}^2/(2B)$, we obtain an energy equation as

$$\frac{d}{dt}\left(\frac{1}{2}m_e v^2 - \mu B\right) = -e\frac{\boldsymbol{E}\cdot\boldsymbol{B}}{B}v_{\parallel}. \tag{4}$$

We eliminate $\tilde{\boldsymbol{v}}$ in Eq. (1) by time averaging. The parallel velocity $v_{\parallel}$ is then related to the infinitesimal length along the field line, $ds = Bdx/B_{x0}$, through

$$v_{\parallel} = \frac{ds}{dt} - \frac{B}{B_{x0}}v_{dx}, \tag{5}$$

where v_{dx} is the x component of the drift velocity. Substituting Eq. (5) in Eq. (4) yields

$$\frac{d}{dt}\left(\frac{1}{2}m_e v^2 - \mu B\right) = -e\frac{\boldsymbol{E}\cdot\boldsymbol{B}}{B_{x0}}\left(\frac{dx}{dt} - v_{dx}\right). \tag{6}$$

Then, using the quantity

$$F(x,t) = -\int^{x}\frac{\boldsymbol{E}(x',t)\cdot\boldsymbol{B}(x',t)}{B_{x0}}dx', \tag{7}$$

we can put Eq. (6) into the following form

$$\frac{d}{dt}\left(\frac{1}{2}m_e v^2 - \mu B - eF\right) = -e\frac{\partial F}{\partial t} - e\frac{\partial F}{\partial x}v_{dx}. \tag{8}$$

We may write the kinetic energy as $m_e v^2/2 = m_e(v_{\parallel}^2 + v_d^2)/2 + \mu B$. Hence, except for the term $m_e v_d^2/2$, the quantity $\varepsilon = m_e v^2/2 - \mu B - eF$ is related to parallel velocity and parallel electric field $E_{\parallel}$. We note that $E_{\parallel}$ is a mixture of longitudinal and transverse electric fields.

Now, we consider perturbations of F such that their time scale is much shorter than the ion gyroperiod with their scale length of the order of the shock width $(\sim c/\omega_{\mathrm{pi}})$.[27–29] We can then neglect the second term on the right-hand side of Eq. (8):

$$\frac{d}{dt}\left(\frac{1}{2}m_e v^2 - \mu B - eF\right) = -e\frac{\partial F}{\partial t}. \tag{9}$$

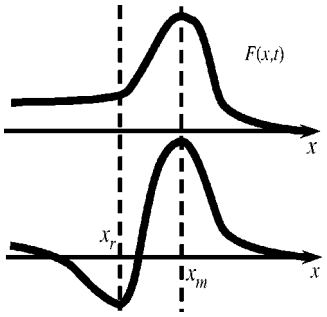

FIG. 1. Model profiles of F. The lower figure shows F with a negative dip around $x=x_r$ at $t=t_r$. In the upper figure for a later time $t>t_r$, F has recovered.

Using Eq. (9), we discuss the energy change of electrons that are reflected at $x=x_r$, near the end of the main pulse, at time $t=t_r$. The quantity F is assumed to take its minimum (negative) value at this x position at this moment; it then recovers for $t>t_r$ (see Fig. 1). In the wave frame (shock normal incident frame), where the upstream plasma flows in the negative x direction with $v_x=-v_{\mathrm{sh}}$, it may be modeled by

$$F(x,t) = F_0(x) + F_1(x,t). \tag{10}$$

The time-independent, main term is $F_0(x)\geqslant 0$, taking its maximum value at $x=x_m(>x_r)$, while the perturbation F_1 is assumed to take the form

$$F_1(x,t) = -a(t)\left[1 + \cos\left(\pi\frac{x-x_r}{x_m-x_r}\right)\right] \tag{11}$$

for $|x-x_r|\leqslant x_m - x_r$; outside this region, $a(t)=0$. Here, $a(t)>0$ and $da/dt<0$ for $t>t_r$. The quantity $F=F_0+F_1$ takes its minimum (negative) value at $x=x_r$, as shown in the lower part of Fig. 1. Then,

$$-e\frac{\partial F_1}{\partial t} < 0 \tag{12}$$

for the region $|x-x_r|\leqslant x_m - x_r$ for $t>t_r$. That is, if an electron is reflected near the end of the main pulse because $F(x_r,t_r)$ is negative, then $F(x,t)$ will be gradually restored around the point $x=x_r$ while the particle moves back from $x=x_r$ to $x=x_m$. During this period, the parallel energy of this particle, $\epsilon = m_e v^2/2 - \mu B - eF$, will thus decrease. As a result, reflected electrons will be trapped. They will not go away ahead of the shock wave. Also, even if $F(x_r,t)>0$ when these electrons return to the point $x=x_r$, they can be reflected there again.

The negative dip of F will not be formed in the main pulse region, where F_0 has large positive values.[1] In front of the main pulse, small negative dips can be generated. Even if some electrons are reflected there, they are not strongly accelerated. It is because there is no large F or electric potential in the upstream region. In the end of the main pulse, on the other hand, F_0 is small and field variations are significant. Hence, negative dips of F can be produced there. Electrons that have been reflected there then gain a great amount of energy from the strong electric fields in the main pulse region.

B. Comparison with previous formulation

In this section, we compare the energy equation in the present paper with that in the previous papers.[1–3] In Ref. 1, an energy conservation form

$$\frac{d}{dt}\left(\frac{1}{2}m_e v^2 - eF + m_e c\frac{E_{y0}}{B_{x0}}v_x\right) = 0 \tag{13}$$

has been derived under the assumption that the wave is perfectly stationary, where E_{y0} is the y component of the electric field in the wave frame. In the drift approximation, Eq. (13) was then written as

$$\frac{d}{dt}\left(\frac{m_e}{2}(v_\parallel^2 + v_d^2) + \mu B - eF + m_e c\frac{E_{y0}}{B_{x0}}v_{gz}\right) = 0, \tag{14}$$

where v_{gz} is the z component of the guiding center velocity. Equations (8) and (14) seem quite different. We show here, however, that they are equivalent when $\partial F/\partial t = 0$.

We recall that $E_y = E_{y0}$ (constant) and $E_z = 0$ in the wave frame, if the wave is stationary. It then follows that

$$m_e c\frac{E_{y0}}{B_{x0}}\frac{dv_z}{dt} = \frac{m_e c}{B_{x0}}\left(E_{y0}\frac{dv_z}{dt} - E_z\frac{dv_y}{dt}\right). \tag{15}$$

The right-hand side is proportional to the x component of $\boldsymbol{E}\times d\boldsymbol{v}/dt$. Using the equation of motion, we find that

$$\boldsymbol{E}\times\frac{d\boldsymbol{v}}{dt} = -\frac{e}{m_e c}\boldsymbol{E}\times(\boldsymbol{v}\times\boldsymbol{B}). \tag{16}$$

Substituting Eq. (1) for $\boldsymbol{v}$ on the right-hand side gives

$$\boldsymbol{E}\times\frac{d\boldsymbol{v}}{dt} = -\frac{e}{m_e c}[(\boldsymbol{E}\cdot\boldsymbol{B})\boldsymbol{v}_d + (\boldsymbol{E}\cdot\boldsymbol{B})\tilde{\boldsymbol{v}} - (\boldsymbol{E}\cdot\tilde{\boldsymbol{v}})\boldsymbol{B}], \tag{17}$$

where the relation $\boldsymbol{E}\cdot\boldsymbol{v}_d = 0$ was used. We time average the x component of Eq. (17) over a gyroperiod. On account of Eqs. (3) and (7), we then have

$$\left\langle \boldsymbol{E}\times\frac{d\boldsymbol{v}}{dt}\right\rangle_x = \frac{eB_{x0}}{m_e c}\frac{\partial F}{\partial x}v_{dx} - \frac{B_{x0}}{m_e c}\frac{d}{dt}(\mu B). \tag{18}$$

We have dropped the term $(\boldsymbol{E}\cdot\boldsymbol{B})\tilde{v}_x$ by the averaging. Equation (15) can thus be written as

$$\left\langle m_e c\frac{E_{y0}}{B_{x0}}\frac{dv_z}{dt}\right\rangle = e\frac{\partial F}{\partial x}v_{dx} - \frac{d}{dt}(\mu B). \tag{19}$$

Since $\langle v_z\rangle = v_{gz}$, we find that Eq. (8) is equivalent to Eq. (14).

Before closing this section, we note, for later use, that for a perfectly stationary, one-dimensional wave, we can derive an energy conservation form that is valid for relativistic particles in the wave frame,[1]

$$m_e c^2\gamma - eF + cp_z\frac{E_{y0}}{B_{x0}} = \varepsilon. \tag{20}$$

Here, γ is the Lorentz factor, p_z is the z component of the momentum, E_{y0} is the constant electric field in the y direction, and the energy ε is constant.

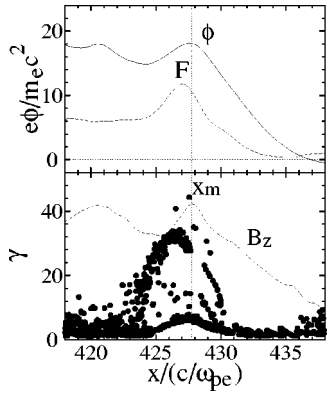

FIG. 2. Snapshot of field profiles and electron phase space (x,γ).

III. SIMULATIONS

We study electron motions in a shock wave by using a one-dimensional (one space coordinate and three velocities), relativistic, electromagnetic particle code with full ion and electron dynamics. As in the theory in Sec. II, the shock wave propagates in the x direction in an external magnetic field $\boldsymbol{B}_0 = B_0(\cos\theta, 0, \sin\theta)$. For the method of particle simulations and shock waves, see Refs. 1, 6, and 30.

The simulation parameters are as follows: The total system length is $L = 4096\Delta_g$, where Δ_g is the grid spacing; the numbers of ions and electrons are $N_i = N_e = 262\,144$; the mass ratio is $m_i/m_e = 100$; the propagation angle is $\theta = 45°$; the ratio of gyrofrequency and plasma frequency of electrons is $\omega_{ce}/\omega_{pe} = 3.0$ in the upstream region; the light speed is $c/(\omega_{pe}\Delta_g) = 4.0$; and the electron and ion thermal velocities in the upstream region are $v_{Te}/(\omega_{pe}\Delta_g) = 0.23$ and $v_{Ti}/(\omega_{pe}\Delta_g) = 0.023$, respectively. The Alfvén speed is then $v_A/(\omega_{pe}\Delta_g) = 1.2$. The time step is $\omega_{pe}\Delta t = 0.02$.

Figure 2 displays a snapshot of field profiles and electron phase space (x,γ) of a shock wave with a propagation speed $v_{sh} = 2.06v_A$. The values of F and ϕ are set to be zero at $x = \infty$. The fields ϕ, F, and B_z take their maximum values around $x = x_m$. In the main pulse region near $x = x_m$, there are many high-energy trapped electrons.[1–3]

The values of $F(x)$ are positive at any points in this figure. When a negative dip of F is formed in the end of the main pulse, however, some electrons are reflected there and then trapped. As shown in Fig. 3, the number of trapped electrons increases with time, suggesting that trapped electrons are hardly detrapped. Its number rapidly goes up some-

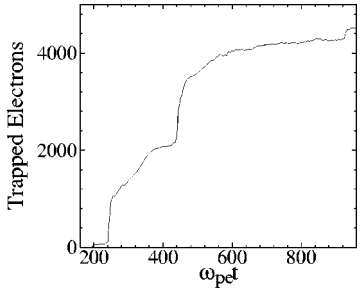

FIG. 3. Time variation of the number of trapped electrons.

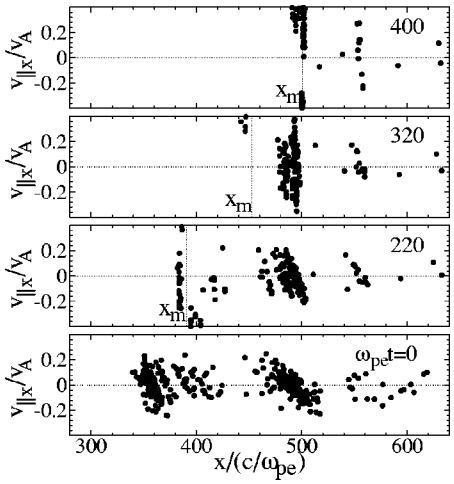

FIG. 4. Phase space plots $(x, v_{\|x})$ of electrons that have been trapped by the end of the simulation. The dotted vertical lines indicate the position $x=x_m$.

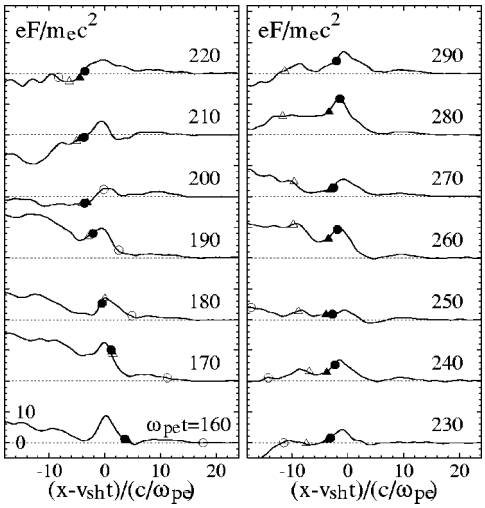

FIG. 5. Profiles of F. Passing and reflected electrons are also shown with circles and triangles.

times, which implies that large negative dips are formed at those moments. Figure 4 shows electron phase space plots $(x, v_{\|x})$ at four different times, where $v_{\|x}$ is the x component of the parallel velocity, $v_{\|x}=(\boldsymbol{v}\cdot\boldsymbol{B})B_{x0}/B^2$. We have plotted the electrons that are trapped by the end of the simulation, $\omega_{pe}t=1000$. The dotted vertical lines indicate the position $x=x_m$. At $\omega_{pe}t=0$, we find rather large bunches around $x/(c/\omega_{pe})=360$ and $x/(c/\omega_{pe})=490$. (There exist many particles other than these; particles are uniformly distributed initially. From the simulation data, we identified the particles that were trapped by the end of the simulation. We selected and plotted here these particles.) In each bunch, high $v_{\|x}$ particles tend to have smaller x, having oblique stripe structure. This indicates that the x positions of these particles will concentrate at a later time; if F is negative there at this moment, many of them would be reflected. Indeed, the particles of the left bunch have nearly the same x position $[x/(c/\omega_{pe})\simeq 382]$ at $\omega_{pe}t=220$ and, at this moment, encounter a negative dip of F; Fig. 3 indicates that the number of trapped electrons rapidly rises around this time. The particles of the right bunch are at nearly the same position, $x/(c/\omega_{pe})=500$, at $\omega_{pe}t=400$. Immediately after this moment, they meet another dip.

Figure 5 shows the evolution of $F(x,t)$ around the main pulse. Near the end of the main pulse, F becomes negative from $\omega_{pe}t=200$ to $\omega_{pe}t=230$ and then recovers to positive values. The x positions of four electrons are plotted on the lines of F. The particles denoted by white and closed triangles and by closed circle enter the shock wave at nearly the same time, $\omega_{pe}t\simeq 160$, while the other one denoted by the white circle comes later, entering the wave at $\omega_{pe}t\simeq 180$. All these particles happen to be at the end of the main pulse when F is negative there. Then, the closed circle and triangle are reflected there; they begin to oscillate in the main pulse. The white circle and triangle, however, escape from this region to the downstream region. They passed through the shock wave because they had larger velocities relative to the shock wave than the reflected particles; it is particularly clear for the white circle.

The upper panel of Fig. 6 shows the change in the relativistic energy $\varepsilon=m_ec^2\gamma-eF+cp_zE_y/B_{x0}$ of a reflected electron; that is, the closed circle in Fig. 5. For comparison, we have plotted in the lower panel the time variation of the x position of this particle. We depicted these figures using the quantities in the wave frame, i.e., the frame moving with the velocity v_{sh} relative to the laboratory frame. Because the wave is not perfectly stationary, E_y slightly varies with time. The lower panel clearly indicates that this particle was trapped after the reflection by the wave. (The short period oscillation is due to the gyromotion.) The upper panel shows that the energy ε decreases after the encounter with the shock wave, which leads to the deep trapping.

IV. SUMMARY

We have theoretically and numerically studied the electron reflection and trapping in an oblique shock wave. Electrons can be reflected by a negative dip of $F(=-\int E_{\|}ds)$ in the end of the main pulse. They are then deeply trapped. After the reflection, they do not go away ahead of the shock wave. Also, when they return to the initial reflection point, they do

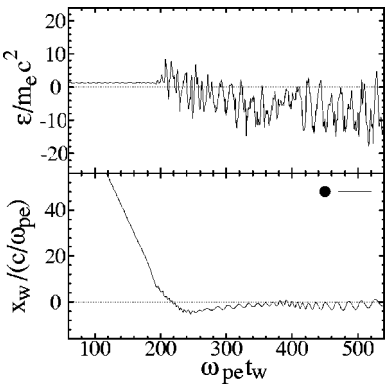

FIG. 6. Time variations of energy $\varepsilon=m_ec^2\gamma-eF+cp_zE_y/B_{x0}$ and position in the wave frame. Here, x_w and t_w denote the position and time in the wave frame.

not pass through this point to the downstream region even if F has recovered to positive values around the reflection point.

To investigate the mechanism of the trapping, we derived an equation for the energy $\varepsilon = m_e v^2/2 - \mu B - eF$, which mainly consists of parallel velocity and parallel electric field. It is then found that if $\partial F/\partial t > 0$ at particle positions after the reflection, the energy ε of a reflected electron decreases. This gives rise to deep trapping.

Particle simulations have demonstrated the electron reflection by a negative dip of F, subsequent recovery of F, decrease of the parallel energy, and trapping.

The trapping and acceleration of electrons have been shown for plasmas in rather strong magnetic fields such that $\omega_{ce}/\omega_{pe} \gtrsim 1$.[1] Hence, these processes are thought to be important in the production of high-energy particles, for instance, in solar magnetic tubes and around pulsars.

As we have seen, the nonstationarity of shock waves plays a crucial role in this mechanism. Even though the propagation of large-amplitude pulses is generally nonstationary, most of the existing wave theories are limited to small-amplitude waves or to stationary waves; we know, for instance, Korteweg–de Vries equation for small-amplitude waves[27–29] and stationary, finite-amplitude, perpendicular wave solutions.[31–33] It is desirable that the theory of nonstationary, large-amplitude waves is developed.

Also, we note that the theory and simulations are both one dimensional in the present and previous studies.[1–3] As future work, it would be important to study multidimensional effects. If the shock front or the external magnetic field has curvature, there may be a mechanism by which some trapped electrons escape from the shock region.

ACKNOWLEDGMENT

This work was carried out by the joint research program of the Solar-Terrestrial Environment Laboratory, Nagoya University.

[1] N. Bessho and Y. Ohsawa, Phys. Plasmas **6**, 3076 (1999).
[2] N. Bessho and Y. Ohsawa, Phys. Plasmas **7**, 4004 (2000).
[3] N. Bessho and Y. Ohsawa, Phys. Plasmas **9**, 979 (2002).
[4] D. Biskamp and H. Welter, Nucl. Fusion **12**, 663 (1972).
[5] D. W. Forslund, K. B. Quest, J. U. Brackbill, and K. Lee, J. Geophys. Res., [Oceans] **89**, 2142 (1984).
[6] Y. Ohsawa, Phys. Fluids **28**, 2130 (1985).
[7] B. Lembege and J. M. Dawson, Phys. Fluids B **1**, 1001 (1989).
[8] R. L. Tokar, S. P. Gary, and K. B. Quest, Phys. Fluids **30**, 2569 (1987).
[9] R. Z. Sagdeev, in *Reviews of Plasma Physics*, edited by M. A. Leontovich (Consultants Bureau, New York, 1966), Vol. 4, pp. 23–91.
[10] R. Z. Sagdeev and V. D. Shapiro, Zh. Eksp. Teor. Fiz. Pis'ma Red. **17**, 387 (1973) [JETP Lett. **17**, 279 (1973)].
[11] Y. Ohsawa, J. Phys. Soc. Jpn. **59**, 2782 (1990).
[12] M. A. Lee, V. D. Shapiro, and R. Z. Sagdeev, J. Geophys. Res., [Oceans] **101**, 4777 (1996).
[13] T. Katsouleas and J. M. Dawson, Phys. Rev. Lett. **51**, 392 (1983).
[14] V. D. Shapiro and D. Üçer, Planet. Space Sci. **51**, 665 (2003).
[15] M. Toida and Y. Ohsawa, J. Phys. Soc. Jpn. **64**, 2036 (1995).
[16] M. Toida and Y. Ohsawa, Sol. Phys. **171**, 161 (1997).
[17] T. P. Armstrong, G. Chen, E. T. Sarris, and S. M. Krimigis, in *Study of Traveling Interplanetary Phenomena*, edited by M. A. Shea and D. F. Smart (Reidel, Dordrecht, 1977), p. 367.
[18] R. B. Decker, Space Sci. Rev. **48**, 195 (1988).
[19] K. Maruyama, N. Bessho, and Y. Ohsawa, Phys. Plasmas **5**, 3257 (1998).
[20] T. Masaki, H. Hasegawa, and Y. Ohsawa, Phys. Plasmas **7**, 529 (2000).
[21] S. Usami, H. Hasegawa, and Y. Ohsawa, Phys. Plasmas **8**, 2666 (2001).
[22] S. Usami and Y. Ohsawa, Phys. Plasmas **9**, 1069 (2002).
[23] S. Usami and Y. Ohsawa, Phys. Plasmas **11**, 918 (2004).
[24] H. Hasegawa, S. Usami, and Y. Ohsawa, Phys. Plasmas **10**, 3455 (2003).
[25] S. Usami and Y. Ohsawa, Phys. Plasmas **11**, 3203 (2004).
[26] G. Schmidt, *Physics of High Temperature Plasmas* (Academic, New York, 1979), Chap. 2.
[27] C. S. Gardner and G. K. Morikawa, Commun. Pure Appl. Math. **18**, 35 (1965).
[28] T. Kakutani, H. Ono, T. Taniuti, and C. C. Wei, J. Phys. Soc. Jpn. **24**, 1159 (1968).
[29] Y. Ohsawa, Phys. Fluids **29**, 1844 (1986).
[30] P. C. Liewer, A. T. Lin, J. M. Dawson, and M. Z. Caponi, Phys. Fluids **24**, 1364 (1981).
[31] J. H. Adlam and J. E. Allen, Philos. Mag., Suppl. **3**, 448 (1958).
[32] L. Davis, R. Lüst, and A. Schlüter, Z. Naturforsch. A **13**, 916 (1958).
[33] Y. Ohsawa, Phys. Fluids **29**, 2474 (1986).